DFT/TD-DFT ANALYSIS OF 2-CHLORO-7-METHYLQUINOLINE-3-CARBALDEHYDE USING COMPUTER COMPUTING METHOD

Nihal KUŞ iD

Department of Physics, Science Faculty, Eskisehir Technical University, 26470, Eskisehir, Turkey

ABSTRACT

Quinolines are the essence of many natural products, drugs and were found in synthetic compounds. Quinoline derivatives containing a quinoline ring are used in a variety of biological and pharmaceutical activities, e.g. anticancer, antibacterial, antifungal, antiplasmodial, antihistamine, antimalarial and antituberculosis. In this study, 2-Chloro-7-Methylquinoline-3-Carbaldehyde (ClMQC) molecule, which is a quinoline derivative, was selected and analyzed. The stable structures of ClMQC molecule with minimum energy were investigated by density functional theory (DFT) together with B3LYP/6-311++G(d,p) method. It was seen that there are two different conformers (*trans* and *cis*) with minimum energy in the scanning made depending on the C─C─C=O dihedral angle. As a result of the calculation with the B3LYP/6-311++G(d,p) level, the energy difference (ΔE+ZPV) between the two conformers was calculated as 14.60 kJ mol^{-1}. Oscillator strength and excitation energies were analyzed by calculating the time-dependent DFT (TD-DFT). The energy differences between the excited energy levels are given in the graph. This was done by adding the ground state energies of both conformers. The energy corresponding to HOMO-LUMO was calculated to correspond to the $S_0 \rightarrow S_2$ transition for both conformers. The excitation energy values were calculated as 3.75 and 3.84 eV for *trans* and *cis*, respectively.

Keywords: 2-Chloro-7-Methylquinoline-3-Carbaldehyde, DFT/TD-DFT, Excitation energies, HOMO-LUMO

1. INTRODUCTION

Quinoline (benzo [b] pyridine) is an aromatic heterocyclic compound characterized by a bicyclic structure consisting of a pyridine ring attached to a benzene ring. Quinoline, whose molecular structure is C9H7N, is the simplest member of its family. Quinoline is an important heterocyclic alkaloid obtained from coal tar in 1834 by Runge [1]. Quinoline, which is very soluble in organic solvents but very slightly in water, has a pungent smell and is colorless. It has wide application areas in medicine, pharmacy, industry and synthetic organic chemistry. For the first time, quinoline and pyrazole were synthesized by the German chemist Ludwig Knorr in 1884 [2]. Quinoline and compounds containing quinoline rings in their structures are one of the most important classes of heterocyclic compounds due to their biological activities such as antibacterial [3], anticancer [4-5], antifungal [6-7] and antimalarial. Chloroquine, quinine, mefloquine and amodiaquine are synthetic quinoline compounds used in antimalarial drugs [8-11]. Chloroquine, from the 4-aminoquinoline class is commonly used in drugs for the treatment of malaria and rheumatoid arthritis [12]. The quinoline derivative used in the treatment of malaria is quinine [(R)-(6-methoxyquinolin-4-yl)((2S,4S,8R)-8-vinylquinuclidin-2-yl)methanol [13]. It has also been used as an antibacterial agent since 1963, and pharmacological quinolone derivatives are synthesized in the chemical field. Quinolone derivatives (fluoroquinolones), which are quinoline derivatives, are also used as antibiotic drugs [14]. Suitable several new synthesis methods for certain 4-hydroxyquinoline and 4-hydroxy-5,6-benzoquinoline derivatives have been developed and reported by Gould et al in 1939 [15].

Madapa *et al* have reviewed the literature on advances in the synthesis of quinolines and quinoline cyclic ring systems since 2005 [16]. No study has been found so far regarding the structure and properties of the MDQC molecule, which is the quinoline derivative studied, and it has been researched and analyzed for the first time.

In our previous studies, the molecular structure and physical properties of quinoline derivatives (5-hydroxyquinoline [17], 3-quinolinecarboxaldehyde [18], 4-chloro-7-iodoquinoline-3-carboxylate [19], 4-oxo-7-methylquinoline-3-carboxylate, 4-Hydroxy-5-methylquinoline-3-carboxylate [20]) were investigated by matrix isolation spectroscopy and reported using computational density functional theory (DFT) and time-dependent DFT (TD-DFT).

In this study, we focused on 2-Chloro-7-Methylquinoline-3-Carbaldehyde (ClMQC). DFT/TD-DFT methods and Natural bond orbital (NBO) analysis were used theoretically and extensively to elucidate the molecule. The results of the calculations using the Gaussian 09 program were analyzed and discussed. The ClMQC (*trans* and *cis*) conformers were fully optimized at ground state equilibrium and theoretically investigated using DFT/B3LYP-6-311++G(d,p) theory level. The low energy excited state energies of the molecule were calculated by TD-DFT and the singlet state HOMO-LUMO orbitals were analyzed computationally.

2. MATERIAL AND METHODS

The geometry optimizations of the molecule were performed at the DFT/B3LYP [it is a 3-parameter Becke mixed model with Lee-Yang-Parr (LYP) correlation energy]/6-311++G(d,p) theory level with the restricted method for closed-shell systems using the GAUSSIAN 09 computer program package [21-23]. All theoretical calculations were performed in the gas phase.

NBO has performed accordingly to Weinhold and co-workers, using NBO 3.1 [24-25], as implemented in Gaussian 09. Energies of the low-energy excited states were calculated using the time-dependent density functional theory (TD-DFT) [26-27] at the B3LYP/6-311++G(d,p) level of approximation.

3. RESULTS AND DISCUSSION

Two conformers (*trans* and *cis*) of ClMQC in the ground state (S_o) were found at minimum energy by calculating at DFT/B3LYP/6-311++G(d,p) level of theory (Figure 1). Both conformers are planar and have C_s symmetry. *Trans* and *cis* conformers at minimum energy were obtained by scanning the dihedral angle of C4−C3−C=O in 15-degree steps
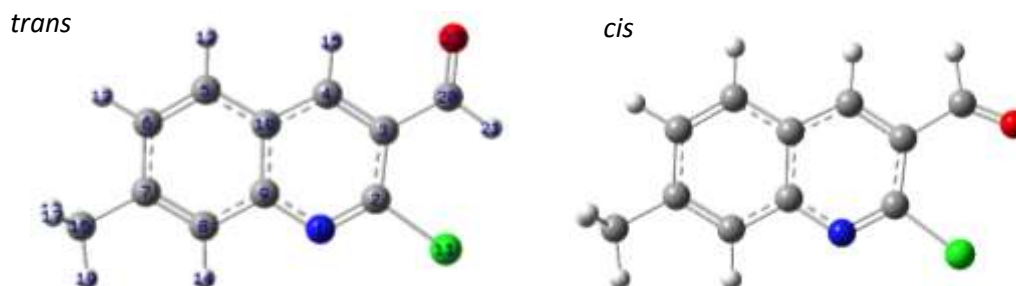

Figure 1. Structure of *trans* and *cis* conformers of ClMQC in the ground state (S_o) calculated at the B3LYP/6-311++G(d,p) level of approximation.

As seen in Table 1 below, according to the results calculated at the B3LYP/6-311++G(d,p) level, *cis* conformer was found to be at higher energy than *trans* conformer about ΔE=13.90 kJ mol^{-1}; ΔE(0)=13.41 kJ mol^{-1}; ΔG°=12.93 kJ mol^{-1} (ΔE, ΔE(0) and ΔG° are relative electronic energy, zero point corrected electronic energy and Gibbs energy).

Table 1. Calculated relative electronic energy (with and without zero-point vibrational energy), Gibbs energy and dipole moment for *trans* and *cis* conformer, obtained from B3LYP/6-311++G(d,p) level.

Energies	*trans*	*cis*
ΔE (kJ mol^{-1})	0	13.90
ΔE(ZPV) (kJ mol^{-1})	0	13.41
ΔG° (kJ mol^{-1})	0	12.93
m (debye)	4.5781	6.4067

There is only one internal rotation defined around the C−C bond belonging to the aldehyde group attached to the ring The potential energy profile of the minimum energy conformers resulting from incrementing in steps of 15 degrees corresponds to rotation around $C_3−C_{20}$ bond is shown in Figure 2. According to the 2D potential energy map, with the rotation of the aldehyde group of ClMQC, conformers called *trans* (internal rotation 0°) and *cis* (internal rotation 180°) were expected at minimum energy, and as we mentioned above about energies, the *trans* form was the most stable conformer.
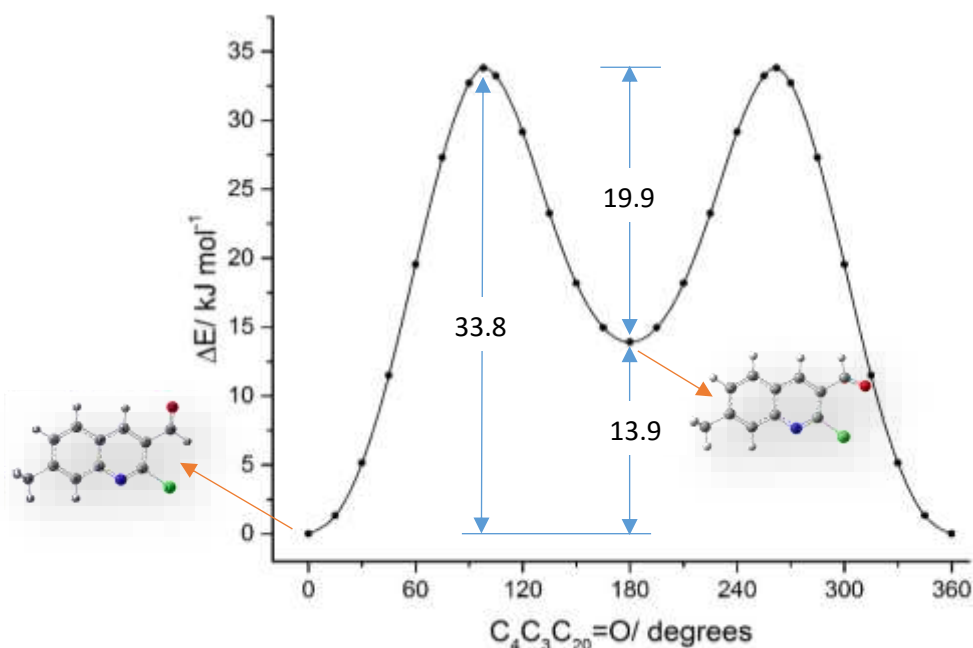
Figure 2. Potential energy profiles calculated by B3LYP/6-311++g(d,p) level for rotation about C–C bond for ClMQC (adopted atom numbers are given in Figure 1).

When analyzing the potential energy profile (Figure 2), the barrier energy produced by the rotation around the C−C bond connecting the aldehyde group to the ring is about 33.8 kJ mol^{-1} (19.9 kJ mol^{-1} in opposite direction) taken from the bottom of the potential well. In our previous study, the structure of the N- Salicyliden- p- carboxyaniline molecule was reported and the barrier energy was found to be approximately 30 kJ mol-1 in the potential energy profile calculated considering the C−C bond. This amount of energy allowed us to trap two forms of E-enols (forms I and II) in the matrix at room temperature [28].
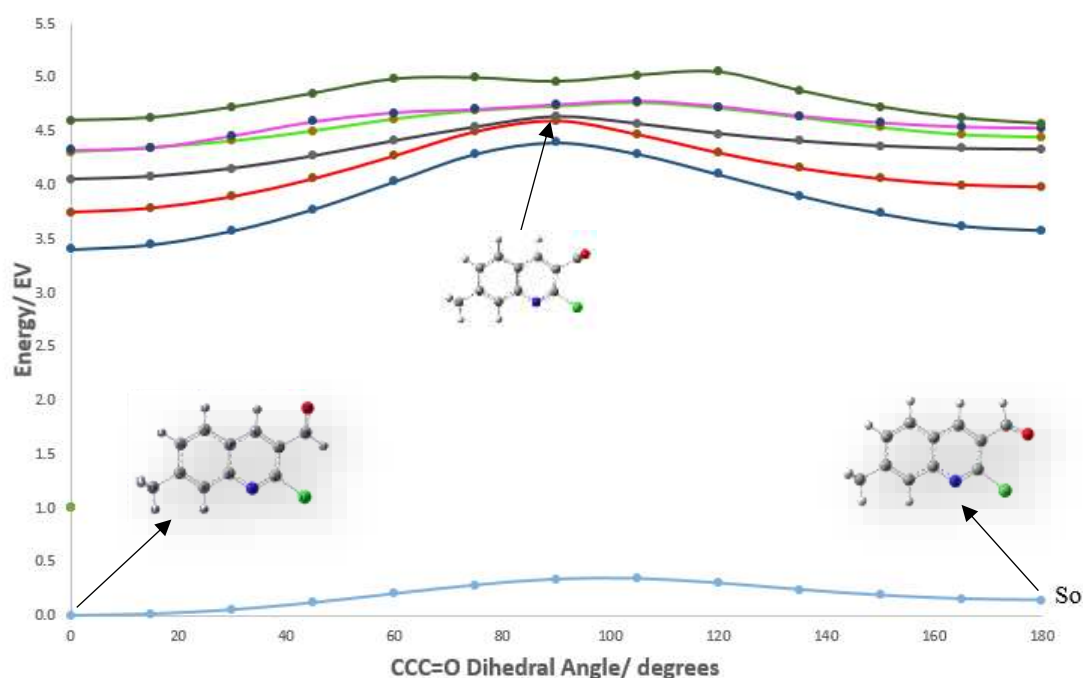
Figure 3. The lowest six energy singlet states of ClMQC calculated at the TD-DFT/B3LYP/6-311++G(d,p) level. S_0; ground state (light blue), S_1; (dark blue), S_2; (red), S_3; (grey), S_4; (light green), S_5; (pink), S_6; (dark green).

In the case of internal rotation of the C−C bond of the aldehyde group of ClMQC, the electronic vertical transition excitations from S_0 to S_1, S_2, S_3, S_4, S_5 and S_6 were calculated at the TD-DFT(B3LYP)/6-311++G(d,p) level of theory and presented graphically in Figure 3. In the TD-DFT graph, it is shown that the S_2 (red) singlet state is from HOMO to LUMO excitation and the energy value of this range is around 3.75 eV for *trans* and 3.80 eV for *cis* conformer.

Table 2. TD-DFT results for the *trans* and *cis* of ClMQC were calculated using B3LYP/6-311++G(d,p) level.

State	type	λ/nm	E/eV	f	dom.orb.cont(%)
ClMQC-*trans*					
S_1	HOMO$_{-2}$-LUMO	364.26	3.40	0.0000	67
S_2	HOMO-LUMO	330.82	3.75	0.0171	31
S_3	HOMO$_{-1}$-LUMO	305.70	4.06	0.1666	54
S_4	HOMO$_{-3}$-LUMO	287.92	4.31	0.0005	68
S_5	HOMO$_{-2}$-LUMO$_{+1}$	286.46	4.33	0.0005	64
S_6	HOMO-LUMO$_{+1}$	269.48	4.60	0.2991	50
ClMQC-*cis*					
S_1	HOMO$_{-1}$-LUMO	360.78	3.44	0.0000	66
S_2	HOMO-LUMO	322.89	3.84	0.0134	62
S_3	HOMO$_{-2}$-LUMO	296.14	4.19	0.1092	52
S_4	HOMO$_{-3}$-LUMO	288.32	4.30	0.0008	60
S_5	HOMO$_{-1}$-LUMO$_{+1}$	282.55	4.39	0.0003	57
S_6	HOMO$_{-3}$-LUMO$_{+1}$	280.10	4.43	0.0004	69

This direct $S_0 \rightarrow S_2$ transition has the $\pi\pi^*$ character and is considered an ineffective transition with zero oscillator strength for *trans* and *cis*, which is not forbidden. In the graph, it is seen that when the aldehyde group rotates perpendicular to the ring (90°), the energies forming the S_2 (4.26 eV) and S_3 (4.29 eV) states are almost equal, with a very small difference. In other words, the molecule with this symmetry can be in both S_2 and S_3 states when excited with this amount of energy. In this case, the barrier energy is at its maximum, such as 33.8 kJ mol^{-1}.

The transition energy state, transition types, excitation wavelengths (λ), transition energies (E) oscillator strengths (*f*) and dominant orbital contributions are given in Table 2 for *trans* and *cis* conformer of ClMQC. As can be seen from the table, it has been estimated that the oscillator power is high and the excitations due to these transitions will be effective only in the S_3 and S_6 transition states for *trans*. According to the calculations, it was found that the most effective transition for the *cis* form was only in the S3 state, and it was thought that absorption would be more effective on this transition.
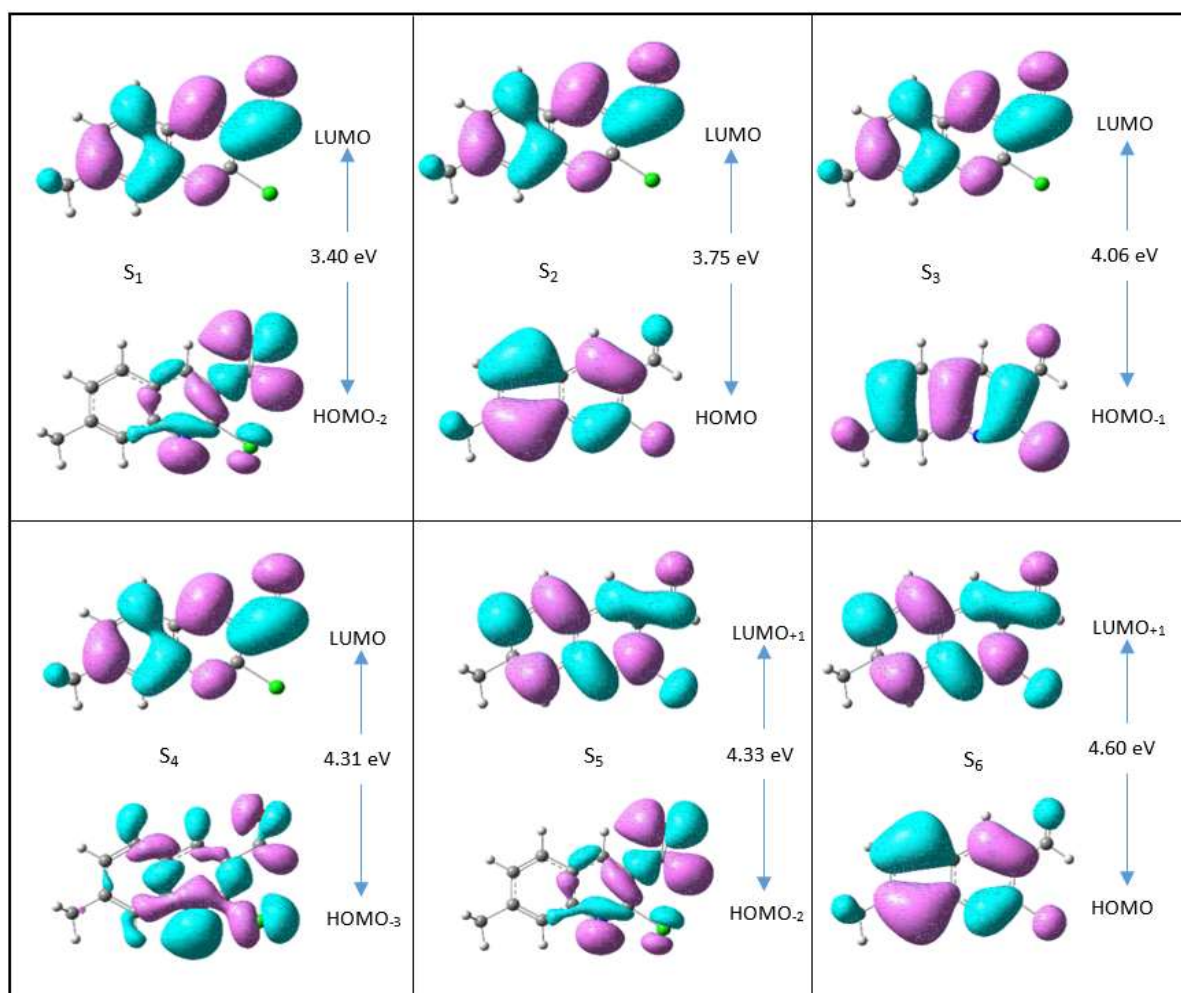
Figure 4. B3LYP/6-311++G(d,p) calculated HOMO and LUMO iso-surfaces (contour is ±0.02 au) for *trans* and its eigenvalues which in the singlet state exhibit a significant oscillator strength also participate in low-energy electronic transitions (as acceptor or donor orbitals) (Table 2).

Figures 4 and 5 show the molecular orbitals for *trans* and *cis* plotted with the Gauss View program with 0.02 isovalues for both phase domains. HOMO and LUMO Molecular orbitals play an important role in determining electronic transitions. The electronic transition with the highest oscillator strength was found in the HOMO-LUMO$_{+1}$ energy range (eigenvalue) and its value is *ca.* 0.30 on *trans*. For the *cis* conformer, this value is smaller, 0.11, which corresponds to the S$_3$ transition and is in the HOMO-2-LUMO energy range. In this case, as can be seen from Table 2, the absorption probability for *trans* in the S$_6$ singlet state is higher and the excitation energy value is calculated to be 4.60 eV. Also, the HOMO-LUMO types for *trans* and *cis* are shown in Figure 4 and Figure 5. When the dominating orbital contribution percentages are taken into account, it is seen that the contribution in the *cis* form is 62% and in the *trans* form this contribution is less, such as 31%.
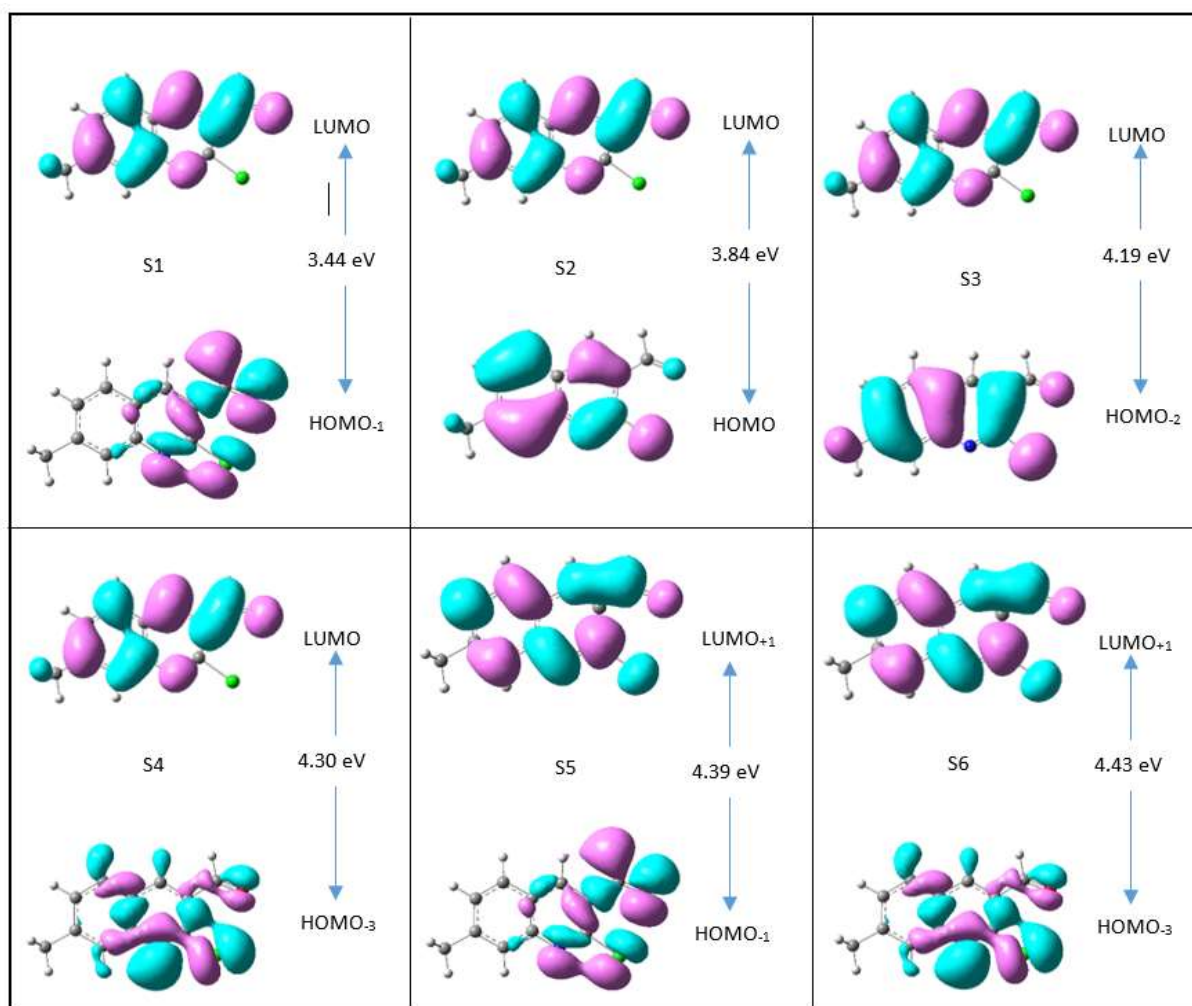

Figure 5. B3LYP/6-311++G(d,p) calculated HOMO and LUMO iso-surfaces (contour is ±0.02 au) for *cis* form and its eigenvalues which in the singlet state exhibit a significant oscillator strength also participate in low-energy electronic transitions (as acceptor or donor orbitals) (Table 2).

The electronic transition with the highest oscillator strength was found in the HOMO-LUMO$_{+1}$ energy range (eigenvalue) and its value is *ca.* 0.30 on *trans*. For the *cis* conformer, this value is 0.11, which corresponds to the S$_3$ transition and is in the HOMO-2-LUMO energy range. In this case, as can be seen from Table 2, the absorption probability for *trans* in the S$_6$ singlet state is higher and the excitation energy value is calculated to be 4.60 eV. Also, the HOMO-LUMO types for *trans* and *cis* are shown in

Figure 3 and Figure 4. Considering the orbital contributions, the HOMO-LUMO energy difference is 3.75 eV for the *trans* conformer, while this value is 3.84 eV for the *cis* conformer. It was found that the transition from HOMO to $LUMO_{+1}$ in vertically calculated electronic energies were at the highest energy, and 4.60 and 4.43 eV for *trans* and *cis*. In both conformers, the HOMO orbital is more localized in the rings, while the LUMO orbitals are localized over the entire molecule.

4. CONCLUSIONS

The structure and electronic properties of ClMQC were investigated by DFT/TD-DFT and NBO methods. According to the potential energy profile obtained by the internal rotation of the CC bond of the aldehyde group of ClMQC, calculated the theory level of DFT/B3LYP/6-311++G(d,p). Two conformers of ground-state (S_0) ClMQC, *trans* and *cis* were found. Considering the zero-point energy, the *trans* conformer was more stable than the *cis* form by 13.41 kJ mol^{-1}. By calculating the electronic transition energies with TD-DFT, it was found that the highest transition energy is in the $S_0{\rightarrow}S_1$ state and this situation corresponds to the $HOMO\text{-}LUMO_{+1}$ transition. The energy value is 4.60 eV, and the oscillator strength was found to be the most effective value of about 0.30 for *trans* form. The most efficient transition for the *cis* form was in the S_3 singlet state, corresponding to the $HOMO_{-2}\text{-}LUMO$ transition. In this case, the oscillator power was about 0.11 and the transition energy was calculated as 4.19 eV. Considering the transitions in the HOMO-LUMO energy range, transition corresponded to the S_2 state for both conformers and the energies were calculated as 3.75 eV for *trans* and 3.84 eV for *cis*.

ACKNOWLEDGMENT

CONFLICT OF INTEREST

The author stated that there are no conflicts of interest regarding the publication of this article.

REFERENCES

[1]   Runge FF. Ueber einige Produkte der Steinkohlendestillation. Ann Physik Und Chem, 1834; 31: 65-78.

[2]   Knorr L. Synthetische Versuche mit dem Acetessigester. Justus Liebigs Annalen der Chemie 1887: 238: 137-219.

[3]   Chevalier J, Bredin J, Mahamoud A, Malléa M, Barbe J, Pagès JM. Inhibitors of antibiotic efflux in resistant Enterobacter aerogenes and Klebsiella pneumoniae strains. Antimicrob Agents Chemother 2004; 48(3): 1043–1046.

[4]   Dassonneville L, Lansiaux A, Wattelet A, Wattez N, Mahieu C, Van Miert S, Pieters L, Bailly C. Cytotoxicity and cell cycle effects of the plant alkaloids cryptolepine and neocryptolepine: relation to drug-induced apoptosis. Eur J Pharmacol 2000; 409(1): 9-18.

[5]   Solomon VR, Lee H. Chloroquine and its analogs: A new promise of an old drug for effective and safe cancer therapies. Eur J Pharmacol 2009; 625: 220−33.

[6]   Vargas LY, Castelli MV, Kouznetsov VV, Urbina JM, Lopez SN, Sortino M, Enriz RD, Ribas JC, Zacchino S. In vitro Antifungal Activity of New Series of Homoallylamines and Related Compounds with Inhibitory Properties of the Synthesis of Fungal Cell Wall Polymers. Bioorg Med Chem 2003; 11: 1531−1550.

[7]   Ablordeppey SY, Fan P, Li S, Clark AM, Hufford CD. Substituted Indoloquinolines as New Antifungal Agents. Bioorg Med Chem 2002, 10, 1337−1346.

[8]   Wiesner J, Ortmann R, Jomaa H and Schlitzer M. New antimalarial drugs. Angew Chem Int Ed Engl 2003; 42: 5274−529.

[9]   Foley M, Tilley L. Quinoline antimalarials: mechanisms of action and resistance. Int J Parasitol 1997; 27(2): 231−40.

[10]   Vlok MC. Artemisinin-Quinoline Hybrids: Design, Synthesis and Antimalarial Activity. Ph.D. Thesis, North-West University, Potchefstroom, 2013.

[11]   Vandekerckhove S, D'hooghe M. Quinoline-based antimalarial hybrid compounds. Bioorg Med Chem 2015; 23: 5098–5119.

[12]   Augustijns P, Geusens P and Verbeke N. Chloroquine levels in blood during chronic treatment of patients with rheumatoid arthritis. Eur J Clin Pharmacol 1992; 42: 429−433.

[13]   Dondorp A, Nosten F, Stepniewska K, Day N, White N. South East Asian Quinine Artesunate Malaria Trial (SEAQUAMAT) group. Artesunate versus quinine for treatment of severe falciparum malaria: a randomized trial. Lancet 2005; 366: 717−25.

[14]   Paton JH, Reeves DS. Fluoroquinolone antibiotics. Microbiology, pharmacokinetics and clinical use. Drugs 1988; 36(2): 193−228.

[15]   Gordon GR and Walter A. Jacobs Synthesis of Substituted Quinolines and 5,6-Benzoquinolines. J Am Chem Soc 1939; 61: 2890–2895.

[16]   Madapa S, Tusi Z, Batra S. Advances in the Synthesis of Quinoline and Quinoline-Annulated Ring Systems. Curr Org Chem 2008; 12: 1116−1183.

[17]   Kuş N, Sagdinc S, Fausto R. Infrared Spectrum and UV-Induced Photochemistry of Matrix-Isolated 5-Hydroxyquinoline. J Phys Chem A 2015; 119(24):6296−308.

[18]   Kuş N, Henriques MS, Paixão JS, Lapinski L and Fausto R. Crystal Structure, Matrix-Isolation FTIR, and UV-Induced Conformational Isomerization of 3-Quinolinecarboxaldehyde. J Phys Chem A 2014; 118 (38): 8708−8716.

[19]   Horta PC, Henriques MSC, Kuş N, Paixão JA, O'Neill PM, Cristiano MLS, Fausto R. Synthesis, structural and conformational analysis, and IR spectra of ethyl 4-chloro-7-iodoquinoline-3-carboxylate Tetrahedron 2015; 71: 7583−7592.

[20]   Horta P, Kuş N, Henriques MS, Paixão JA, Coelho L, Nogueira F, O'Neill PM, Fausto R, Cristiano ML. Quinolone-Hydroxyquinoline Tautomerism in Quinolone 3-Esters. Preserving the 4-Oxoquinoline Structure To Retain Antimalarial Activity. J Org Chem 2015; 80(24): 12244−57.

[21]   Frisch MJ *et al.* Gaussian 09, Revision A.0.2. Gaussian Inc, Wallingford CT, 2009.

[22]   Becke AD. Density-functional exchange-energy approximation with correct asymptotic behavior. Phys Rev A 1988; 38: 3098–3100.

[23]   Lee C, Yang W, Parr RG. Development of the Colle-Salvetti correlation-energy formula into a functional of the electron density. Phys Rev B 1988; 37: 785–789.

[24]   Reed AE, Curtiss LA, Weinhold F. Intermolecular interactions from a natural bond orbital, donor-acceptor viewpoint. Chem Rev 1988; 88: 899–926.

[25]   Weinhold F, Landis CR. Valency and Bonding. A Natural Bond Orbital Donor-Acceptor Perspective. Cambridge University Press: New York, 2005.

[26]   Bauernschmitt R, Ahlrichs R. Treatment of Electronic Excitations Within the Adiabatic Approximation of Time Dependent Density Functional Theory. Chem Phys Lett 1996; 256: 454−464.

[27]   Stratmann RE, Scuseria GE, Frisch MJ. An Efficient Implementation of Time-Dependent Density-Functional Theory for the Calculation of Excitation Energies of Large Molecules. J Chem Phys 1998; 109: 8218−8224.

[28]   Avadanei M, Kuş N, Cozan V and Fausto R. Structure and Photochemistry of N- Salicylidene- p- carboxyaniline Isolated in Solid Argon. J Phys Chem A 2015; 119: 9121−9132.